International Journal of Modern Manufacturing Technologies
ISSN 2067–3604, Vol. V, No. 2 / 2013

THE MODELING AND ANALYSIS OF A PARTIAL LOADS IN THE FANUC AM100IB ROBOT JOINTS

Jerzy Świder[1], Adrian Zbilski [2]

[1]Silesian University of Technology, Faculty of Mechanical Engineering
Institute of Engineering Processes Automation and Integrated Manufacturing System,
ul. Konarskiego 18A/268, 44-100 Gliwice, Poland
[2] Silesian University of Technology, Faculty of Mechanical Engineering
Institute of Engineering Processes Automation and Integrated Manufacturing System,
ul. Konarskiego 18A/268, 44-100 Gliwice, Poland

Corresponding author: Adrian Zbilski, adrian.zbilski@polsl.pl

Abstract: This paper concerns the dynamic model description of the Fanuc AM100iB robot. The model was developed with the usage of the recursive Newton-euler method. The purpose of this work was to supplement the numerical model of the robot with additional subsystems, which calculate the total, resultant and partial values of driving torques, developed on the investigated machine's motors. In addition, this work sought to determine the total, resultant and partial driving torques allowed for performing simulation research into the energy intensity of selected transportation and manipulation processes and their algorithmisation. The obtained results were verified by numerical simulations, performed with the use of the numerical robot model.
Key words: modelling, simulation, loads, robot joint, Newton-Euler method.

1. INTRODUCTION

The dynamic model of the investigated robot was prepared according to the adopted methodology of carrying out research with the machine's energy intensity, taking into consideration the source of its needs for providing energy and the reasons for its losses. One of the reasons, which demands the need to provide energy to the robot's drives are the driving torques, developed on the motors' shafts. The total values of those parameters consist of the values of resultant and partial torques, which result from the action of different types of forces that load the robot's arms. The information about them, at each moment in time during a single robot's movement, allowed an assessment to be made regarding the level of influence of each of them on the total electric energy consumption. These values, which needed the most power and the largest amount of energy to be provided to the robot's drives, will be taken into consideration during future research on methods for reducing energy consumption. To develop the equations of inverse dynamics, two of the most common methods are used: the Lagrange-Euler formalism and the Newton-Euler formalism. In a paper (Hollerbach, 1980), based on the comparison of the results from (Luh et al., 1980) it has been proven that the Newton-Euler method is computationally more effective. Similar results have been proven in another paper (Xiaogeng and Goldenberg, 1990). For this reason, this algorithm was used for developing the equations of the Fanuc AM100iB robot's inverse dynamics. In order to familiarise the reader with the methodology of modelling by the use of this approach, the relevant literature (Yoshikawa, 2003; Craig, 2005) can be consulted. The method is frequently chosen because of its other advantages, these include a simplified and methodical way of describing of equations, which allows for easy algorithmisation and computerisation, and also allows for modifications of the standard procedures. Authors of subsequent works (Boyer and Coifet, 1996) improved the Newton-Euler formalism in order to prepare the dynamic model of a robot's flexible arms. In a fairly recent paper (Luca and Ferrajoli, 2009), the NE method was modified in order to improve the fault-detection in a robot's drives, and errors during unexpected collisions appeared during proprioceptive measurements of position and speed. In this paper, the modification was applied due to the adopted purpose, which was to prepare the system for calculating the total, resultant and partial loads acting on the motors' shafts. An analytical model was performed, also due to the practical meaning. Its implementation requires less calculating power than its numerical equivalent, as in the block diagram.

2. THE MODEL OF THE ROBOT STRUCTURE

2.1 Forward kinematics and its modifications

In the paper, the orientations and positions of local coordinate systems were adopted, according to figure

(Fig. 1a). This configuration results from the directions of rotations used in a real robot and from modified Denavit-Hartenberg notation. The basic DH notation is described in (Craig, 2005).

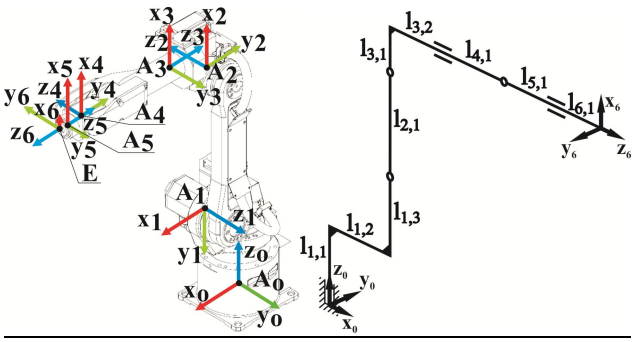

Fig. 1 a.) Adopted robot's local coordinate systems, b.) Phenomenological model of the robot

The DH notation was modified in order to obtain consistency of results calculated both numerically and analytically. Values of parameters of the robot's local coordinates systems are included in Table 1.

Table 1. Parameters of translation and rotation the robot's local coordinate systems.

Nr	Θ_i	λ_i	l_i	α_i
1.	q_1	$l_{1,3}$	$l_{1,2}$	-90
2.	$\left(q_2-\frac{\pi}{2}\right)$	0	$l_{2,1}$	180
3.	q_3	0	l_{3,mod_1}	-90
4.	q_4	$-l_{4,1}$	0	90
5.	q_5	$-l_{5,1,\mathrm{mod}_2}$	0	-90
E.	q_6	$-l_{6,z}$	$\begin{bmatrix} l_{6,x} & l_{6,y} \end{bmatrix}^T$	180

Modification mod_1 modification is responsible for the translation at the beginning of the third local coordinate system to the end of the third robot's arm, according to the equation (2). This translation was obtained by introducing an additional rotation, which does not change the orientation of the transformed local coordinate system, only its position. Modification mod_2 separates operations for changing the position and orientation of a fifth local coordinate system, by the description of translation of the fifth coordinate system as the last operation (3). Those operations, performed in that sequence, imitate the adopted positions and orientation of the fifth local coordinate system.

$$A^3_{2,\mathrm{mod}_1}=\left[\begin{array}{ccc|c} & R^3_2 & & \begin{array}{c} -\cos\left[\left(q_3+\frac{\pi}{2}\right)+a\tan\left(\frac{l_{3,1}}{l_{3,2}}\right)\right]\cdot\sqrt{(l_{3,2})^2+(l_{3,1})^2} \\ -\sin\left[\left(q_3+\frac{\pi}{2}\right)+a\tan\left(\frac{l_{3,1}}{l_{3,2}}\right)\right]\cdot\sqrt{(l_{3,2})^2+(l_{3,1})^2} \\ 0 \end{array} \\ 0 & 0 & 0 & 1 \end{array}\right] \quad (1)$$

$$A^5_{4,\mathrm{mod}_2}=\left[\begin{array}{ccc|c} & R^5_4 & & \begin{array}{c} 0 \\ 0 \\ 0 \end{array} \\ 0 & 0 & 0 & 1 \end{array}\right]\cdot\begin{bmatrix} 1 & 0 & 0 & 0 \\ 0 & 1 & 0 & 0 \\ 0 & 0 & 1 & -l_{5,1} \\ 0 & 0 & 0 & 1 \end{bmatrix} \quad (3)$$

The modifications used allowed full consistency in the position and orientation of the local coordinate systems to be obtained, both in the numerical and analytical model of the investigated robot.

2.2 Geometric relations

In order to describe the geometric relations between the analysed points in the numerical and analytical models, the vectors describing their relative positions were determined. The attachment points of those vectors were the beginnings of local coordinate systems, and the values of their elements were described by the equations (4), (5), (6), (7), (8), (9).

$$r^0_1=\begin{bmatrix} l_{1,2} & -l_{1,3} & 0 \end{bmatrix} \quad (4)$$

$$r^1_2=\begin{bmatrix} l_{2,1} & 0 & 0 \end{bmatrix} \quad (5)$$

$$r^2_3=\begin{bmatrix} l_{3,1} & 0 & -l_{3,2} \end{bmatrix} \quad (6)$$

$$r^3_4=\begin{bmatrix} 0 & -l_{4,1} & 0 \end{bmatrix} \quad (7)$$

$$r^4_5=\begin{bmatrix} 0 & 0 & -l_{5,1} \end{bmatrix} \quad (8)$$

$$r^5_6=\begin{bmatrix} 0 & 0 & l_{6,1} \end{bmatrix} \quad (9)$$

The relations between points describing the beginnings of robot arms and their centres of gravity were described by the equations (10), (11), (12), (13), (14), (15) and the figure (Fig. 2).

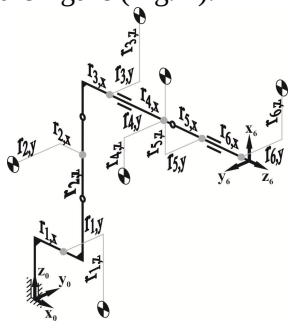

Fig. 2. Adopted designation of coordinates of positions the robot arms' centers of gravity

$$r^0_{c1}=\begin{bmatrix} r_{1,x} & -r_{1,z} & r_{1,y} \end{bmatrix} \quad (4)$$

$$r^1_{c2}=\begin{bmatrix} r_{2,z} & -r_{2,x} & -r_{1,y} \end{bmatrix} \quad (5)$$

$$r^2_{c3}=\begin{bmatrix} r_{3,z} & r_{3,y} & -r_{3,x} \end{bmatrix} \quad (6)$$

$$r^3_{c4}=\begin{bmatrix} r_{4,z} & -r_{4,x} & -r_{4,y} \end{bmatrix} \quad (7)$$

$$r^4_{c5}=\begin{bmatrix} r_{5,z} & r_{5,y} & -r_{5,x} \end{bmatrix} \quad (8)$$

$$r^5_{c6}=\begin{bmatrix} r_{6,z} & -r_{6,y} & r_{6,x} \end{bmatrix} \quad (9)$$

Relations between points describing the ends of robot arms and their centres of gravity are expressed by the equations (16), (17), (18), (19), (20), (21).

$$r_{c1}^{0} = \begin{bmatrix} r_{1,x} & -r_{1,z} & r_{1,y} \end{bmatrix} \quad (16)$$

$$r_{c2}^{1} = \begin{bmatrix} r_{2,z} & -r_{2,x} & -r_{1,y} \end{bmatrix} \quad (17)$$

$$r_{c3}^{2} = \begin{bmatrix} r_{3,z} & r_{3,y} & -r_{3,x} \end{bmatrix} \quad (18)$$

$$r_{c4}^{3} = \begin{bmatrix} r_{4,z} & -r_{4,x} & -r_{4,y} \end{bmatrix} \quad (19)$$

$$r_{c5}^{4} = \begin{bmatrix} r_{5,z} & r_{5,y} & -r_{5,x} \end{bmatrix} \quad (20)$$

$$r_{c6}^{5} = \begin{bmatrix} r_{6,z} & -r_{6,y} & r_{6,x} \end{bmatrix} \quad (21)$$

Some of the elements in the determined vectors have negative signs. This results from describing them in the local coordinate systems at the ends of the arms, looking at them from the back.

3. DYNAMIC MODEL OF THE ROBOT

3.1 Forward recursion

The base element, relative to which all values of kinematic parameters were determined, was the vector of the direction of rotation of the first robot joint z_0, described by the equation (22).

$$z_0 = \begin{bmatrix} 0 & 0 & 1 \end{bmatrix} \quad (22)$$

According to the adopted methodology, the equation describes the kinetic parameters of the selected robot's arms, relative to their centres of gravity.

The base

Relative to the ground, the base is fixed. Therefore, the values of its kinematic parameters are equal to the zero:

$$\omega_0 = \alpha_0 = a_{c,0} = a_{e,0} = 0 \quad (23)$$

Arm 1

According to the adopted methodology, the equations for speed and acceleration were determined using the equations below:

$$\omega_1 = \left(R_1^0 \right)^T \cdot \left(\omega_0 + \dot{q}_1 \cdot z_0 \right) \quad (24)$$

$$\alpha_1 = \left(R_1^0 \right)^T \cdot \left(\alpha_0 + \ddot{q}_1 \cdot z_0 \right) \quad (25)$$

The acceleration of the end of the arm and its centre of gravity is described by equation (26) and (27).

$$a_{e,1} = \left(R_1^0 \right)^T \cdot a_{e,0} + \alpha_1 \times r_{0,1} + \omega_1 \times \left(\omega_1 \times r_{0,1} \right) \quad (26)$$

$$a_{c,1} = a_{e,1} + \alpha_1 \times r_{1,c1} + \omega_1 \times \left(\omega_1 \times r_{1,c1} \right) \quad (27)$$

Based on the obtained equations, the formulas describing the values of the kinematic parameters of the second arm were developed. The equations were determined according to the analogous equations in the first arm.

Arm 2

$$\omega_2 = \left(R_2^1 \right)^T \cdot \left(\omega_1 + \dot{q}_2 \cdot z_0 \right) \quad (28)$$

$$\alpha_2 = \left(R_2^1 \right)^T \cdot \left[\alpha_1 + \ddot{q}_2 \cdot z_0 + \dot{q}_2 \cdot \left(\omega_1 \times z_0 \right) \right] \quad (29)$$

$$a_{e,2} = \left(R_2^1 \right)^T \cdot a_{e,1} + \alpha_2 \times r_{1,2} + \omega_2 \times \left(\omega_2 \times r_{1,2} \right) \quad (30)$$

$$a_{c,2} = a_{e,2} + \alpha_2 \times r_{2,c2} + \omega_2 \times \left(\omega_2 \times r_{2,c2} \right) \quad (31)$$

The rest of the equations describing the values of the kinematic parameters of the robot's arms were prepared.

Arm 3

$$\omega_3 = \left(R_3^2 \right)^T \cdot \left(\omega_2 + \dot{q}_3 \cdot z_0 \right) \quad (32)$$

$$\alpha_3 = \left(R_3^2 \right)^T \cdot \left[\alpha_2 + \ddot{q}_3 \cdot z_0 + \dot{q}_3 \cdot \left(\omega_2 \times z_0 \right) \right] \quad (33)$$

$$a_{e,3} = \left(R_3^2 \right)^T \cdot a_{e,2} + \alpha_3 \times r_{2,3} + \omega_3 \times \left(\omega_3 \times r_{2,3} \right) \quad (34)$$

$$a_{c,3} = a_{e,3} + \alpha_3 \times r_{3,c3} + \omega_3 \times \left(\omega_3 \times r_{3,c3} \right) \quad (35)$$

Arm 4

$$\omega_4 = \left(R_4^3 \right)^T \cdot \left(\omega_3 + \dot{q}_4 \cdot z_0 \right) \quad (36)$$

$$\alpha_4 = \left(P_4^3 \right)^T \cdot \left[\alpha_3 + \ddot{\theta}_4 \cdot z_0 + \dot{\theta}_4 \cdot \left(\omega_3 \times z_0 \right) \right] \quad (37)$$

$$a_{e,4} = \left(R_4^3 \right)^T \cdot a_{e,3} + \alpha_4 \times r_{3,4} + \omega_4 \times \left(\omega_4 \times r_{3,4} \right) \quad (38)$$

$$a_{c,4} = a_{e,4} + \alpha_4 \times r_{4,c4} + \omega_4 \times \left(\omega_4 \times r_{4,c4} \right) \quad (39)$$

Arm 5

$$\omega_5 = \left(R_5^4 \right)^T \cdot \left(\omega_4 + \dot{q}_5 \cdot z_0 \right) \quad (40)$$

$$\alpha_5 = \left(R_5^4 \right)^T \cdot \left[\alpha_4 + \ddot{q}_5 \cdot z_0 + \dot{q}_5 \cdot \left(\omega_4 \times z_0 \right) \right] \quad (41)$$

$$a_{e,5} = \left(R_5^4 \right)^T \cdot a_{e,4} + \alpha_5 \times r_{4,5} + \omega_5 \times \left(\omega_5 \times r_{4,5} \right) \quad (42)$$

$$a_{c,5} = a_{e,5} + \alpha_5 \times r_{5,c5} + \omega_5 \times \left(\omega_5 \times r_{5,c5} \right) \quad (43)$$

Arm 6

$$\omega_6 = \left(R_6^5 \right)^T \cdot \left(\omega_5 + \dot{q}_6 \cdot z_0 \right) \quad (44)$$

$$\alpha_6 = \left(R_6^5 \right)^T \cdot \left[\alpha_5 + \ddot{q}_6 \cdot z_0 + \dot{q}_6 \cdot \left(\omega_5 \times z_0 \right) \right] \quad (45)$$

$$a_{e,6} = \left(R_6^5 \right)^T \cdot a_{e,5} + \alpha_6 \times r_{5,6} + \omega_6 \times \left(\omega_6 \times r_{5,6} \right) \quad (46)$$

$$a_{c,6} = a_{e,6} + \alpha_6 \times r_{6,c6} + \omega_6 \times \left(\omega_6 \times r_{6,c6} \right) \quad (47)$$

The vector products used in the above equations were determined using the description of the matrix of rotational speed as the skew-symmetric matrix. The obtained equations allow the determination of the values of the kinematic parameters of the same points, which exist both in the numerical and analytical models.

3.2 Backward recursion

Backward recursion defines the equations for values of torques acting on the robot's arms. There are torques, whose vectors are attached to the arms' centres of gravity, and its directions must not overlap with the directions of the robot joints' axes. The values acting on the next arms were determined from the last arms to the base. Gravitational acceleration is not directly included in the equations of the NE method, and therefore it was introduced as the effect of the external force acting, attached to the centre of gravity of each arm. That force was the weight. The values of the gravitational acceleration vector are adopted according to the equation (48).

$$g_0 = \begin{bmatrix} 0 & 0 & -g \end{bmatrix}^T \tag{48}$$

The values of external torques and forces acting on the sixth arm are adopted as zero, and in parallel they are the boundary conditions:

$$f_7 = \tau_7 = n_7 = R_7^6 = 0 \tag{49}$$

Arm 6

The values of the gravitational acceleration vector elements were determined according to the equation:

$$g_6 = \left(R_6^0 \right)^T \cdot g_0 \tag{50}$$

The values of forces and torques acting on the arm were calculated according to the equations:

$$f_6 = \left(R_7^6 \right)^T \cdot f_7 + m_6 \cdot \left(a_{c,6} - g_6 \right) \tag{51}$$

$$n_6 = -f_6 \times \left(r_{5,6} + r_{6,c6} \right) + R_7^6 \cdot n_7 + \left[\left(R_7^6 \cdot f_7 \right) \times r_{6,c6} \right] + \\ + I_6 \cdot \alpha_6 + \omega_6 \times \left(I_6 \times \omega_6 \right) \tag{52}$$

Appearing in the equation for torque n_6, the mass moment of inertia was transformed by rotations. Results from the description of local coordinate systems transformations come from DH notation (53).

$$I_6 = R_6^0 \cdot I_6^0 \cdot \left(R_6^0 \right)^T \tag{53}$$

The values of torque, which loads the motor's shaft, were calculated by determining the projection of the torque vector on the direction of the joint's axis, by the projection matrix, and then its reduction by the total ratio of mechanical transmission (54).

$$\tau_6 = \frac{\left(n_6 \right)^T \cdot \left(R_6^5 \right)^T \cdot z_0}{i_6} \tag{54}$$

Analogously, the equations describing the dynamic parameters of the remaining arms were performed.

Arm 5

$$g_5 = \left(R_5^0 \right)^T \cdot g_0 \tag{55}$$

$$f_5 = \left(R_6^5 \right)^T \cdot f_6 + m_5 \cdot \left(a_{c,5} - g_5 \right) \tag{56}$$

$$n_5 = -f_5 \times \left(r_{4,5} + r_{5,c5} \right) + R_6^5 \cdot n_6 + \left[\left(R_6^5 \cdot f_6 \right) \times r_{5,c5} \right] + \\ + I_5 \cdot \alpha_5 + \omega_5 \times \left(I_5 \times \omega_5 \right) \tag{57}$$

$$I_5 = R_5^0 \cdot I_5^0 \cdot \left(R_5^0 \right)^T \tag{58}$$

$$\tau_5 = \frac{\left(n_5 \right)^T \cdot \left(R_5^4 \right)^T \cdot z_0}{i_5} \tag{59}$$

Arm 4

$$g_4 = \left(R_4^0 \right)^T \cdot g_0 \tag{60}$$

$$f_4 = \left(R_5^4 \right)^T \cdot f_5 + m_4 \cdot \left(a_{c,4} - g_4 \right) \tag{61}$$

$$n_4 = -f_4 \times \left(r_{3,4} + r_{4,c4} \right) + R_5^4 \cdot n_5 + \left[\left(R_5^4 \cdot f_5 \right) \times r_{4,c4} \right] + \\ + I_4 \cdot \alpha_4 + \omega_4 \times \left(I_4 \times \omega_4 \right) \tag{62}$$

$$I_4 = R_4^0 \cdot I_4^0 \cdot \left(R_4^0 \right)^T \tag{63}$$

$$\tau_4 = \frac{\left(n_4 \right)^T \cdot \left(R_4^3 \right)^T \cdot z_0}{i_4} \tag{64}$$

Arm 3

$$g_3 = \left(R_3^0 \right)^T \cdot g_0 \tag{65}$$

$$f_3 = \left(R_4^3 \right)^T \cdot f_4 + m_3 \cdot \left(a_{c,3} - g_3 \right) \tag{66}$$

$$n_3 = -f_3 \times \left(r_{2,3} + r_{3,c3} \right) + R_4^3 \cdot n_4 + \left[\left(R_4^3 \cdot f_4 \right) \times r_{3,c3} \right] + \\ + I_3 \cdot \alpha_3 + \omega_3 \times \left(I_3 \times \omega_3 \right) \tag{67}$$

$$I_3 = R_3^0 \cdot I_3^0 \cdot \left(R_3^0 \right)^T \tag{68}$$

$$\tau_3 = \frac{\left(n_3 \right)^T \cdot \left(R_3^2 \right)^T \cdot z_0}{i_3} \tag{69}$$

Arm 2

$$g_2 = \left(R_2^0 \right)^T \cdot g_0 \tag{70}$$

$$f_2 = \left(R_3^2 \right)^T \cdot f_3 + m_2 \cdot \left(a_{c,2} - g_2 \right) \tag{71}$$

$$n_2 = -f_2 \times \left(r_{1,2} + r_{2,c2} \right) + R_3^2 \cdot n_3 + \left[\left(R_3^2 \cdot f_3 \right) \times r_{2,c2} \right] + \\ + I_2 \cdot \alpha_2 + \omega_2 \times \left(I_2 \times \omega_2 \right) \tag{72}$$

$$I_2 = R_2^0 \cdot I_2^0 \cdot \left(R_2^0 \right)^T \tag{73}$$

$$\tau_2 = \frac{(n_2)^T \cdot \left(R_2^1\right)^T \cdot z_0}{i_2} \quad (74)$$

Arm 1

$$g_1 = \left(R_1^0\right)^T \cdot g_0 \quad (75)$$

$$f_1 = \left(R_2^1\right)^T \cdot f_2 + m_1 \cdot \left(a_{c,1} - g_1\right) \quad (76)$$

$$m_1 = -f_1 \times \left(r_{0,1} + r_{1,c1}\right) + R_2^1 \cdot n_2 + \left[\left(R_2^1 \cdot f_2\right) \times r_{1,c1}\right] + + I_1 \cdot \alpha_1 + \omega_1 \times \left(I_1 \times \omega_1\right) \quad (77)$$

$$I_1 = R_1^0 \cdot I_1^0 \cdot \left(R_1^0\right)^T \quad (78)$$

$$\tau_1 = \frac{(n_1)^T \cdot \left(R_1^0\right)^T \cdot z_0}{i_1} \quad (79)$$

3.2 Resultant and partial loads in robot joints

For the aim of determining the values of resultant and partial gravitational loads in the robot joints, zero values of speed and acceleration were adopted. In this way, the influence of the torques of inertial, centrifugal and Coriolis forces was excluded. In order to determine the distribution of torques of gravitational forces from all robot arms acting on all motors' shafts, the values of the masses were zeroed, leaving only geometric transformations and the mass of the analysed arm, according to equation (80).

$$\boldsymbol{\tau}_{\mathbf{i}}^{\mathbf{g}} = NE(\mathbf{q}, 0, 0, m_i), i = 1,...6,\ j = 1,...6 \quad (80)$$

For the aim of determining the values of the resultant and partial centrifugal and Coriolis loads in robot joints, zero values of arms' accelerations and zero values of gravitational acceleration were adopted. In this way, the influence of torques of gravitational and inertial forces were excluded according, to the equation (81).

$$\boldsymbol{\tau}_{\mathbf{i}}^{\mathbf{cc}} = NE(\mathbf{q}, \dot{\mathbf{q}}, 0, m_i, g = 0), i = 1,...6,\ j = 1,...6 \quad (81)$$

In order to determine the values of the resultant and partial inertial loads in robot joints, in the equations for the total torques, zero values of speed and gravitational acceleration were adopted. In this way, the influence of the torques of gravitational and centrifugal and Coriolis forces were excluded according to the equation (82).

$$\boldsymbol{\tau}_{\mathbf{i}}^{\mathbf{in}} = NE(\mathbf{q}, 0, \ddot{\mathbf{q}}, m_i, g = 0), i = 1,...6,\ j = 1,...6 \quad (82)$$

Analogously to the distribution of the weights of all the arms on all of the motors' shafts, the distribution of all centrifugal and Coriolis and inertial forces were determined, by zeroing masses of the excluded arms.

3. NUMERICAL MODEL OF THE ROBOT

3.1 Block diagram

The numerical model of the Fanuc AM100iB robot was performed as a block diagram, by the use of Simulink software with the SimMechanics Toolbox. The model defines the positions of the centres of gravity, the main mass moments of inertia, the ratios of the mechanical transmissions, the lengths of the arms and the types of kinematic couples. The model is driven by ideal sources of torques in each joint, whose values are calculated by the use of a separate control system. In the robot joints, the viscous friction resistive torques act. These are responsible for damping the robot's movements (Fig. 3).

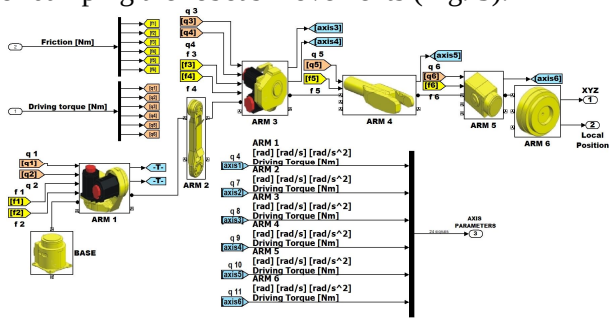

Fig. 3. The first layer of block diagram of the numerical robot model

The prepared model is equipped with a system for generating a reference trajectory, a linear interpolator, a system for calculating inverse kinematics, a system for speed profile generation of a robot's TCP point (Świder and Zbilski, 2013), setpoint-tracking controllers with a cascade structure and feed forward loops. The described systems are responsible for calculating the values of the driving torques, which have to be developed by the numerical robot models drives. Figure (4) presents a view of the connections between the numerical and analytical robot model, the control system and the system calculating the viscous friction torque.

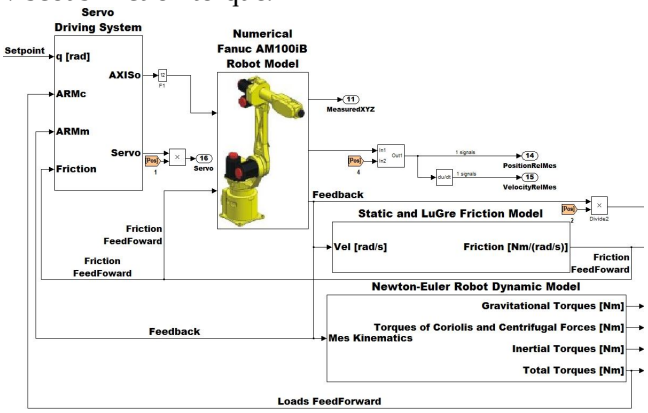

Fig. 4. The view of connections between subsystems controlling the work of numerical and analitycal robot model

4. NUMERICAL VERIFICATION

4.1 Input data

Numerical verification of the performed numerical and analytical models consisted of a comparison between the obtained results from both models, which were extracted after setting the same input data. The values of the dynamic parameters of the investigated robot were determined based on statistical analysis. The analysed trajectory of movement was presented in figure (Fig. 5) and (Fig. 6). These were analysed movements between points A,B and C, see Table 2.

Table 2. The coordinates of set points and rotations of the last local coordinate systems

Pt.	Pos. X, mm	Pos. Y, mm	Pos.Z, mm	Rotat. X, °	Rotat. Y, °	Rotat. Z, °
A	300	600	100	0	60	90
B	600	-500	600	-60	-89	0
C	700	500	-400	0	0	-90

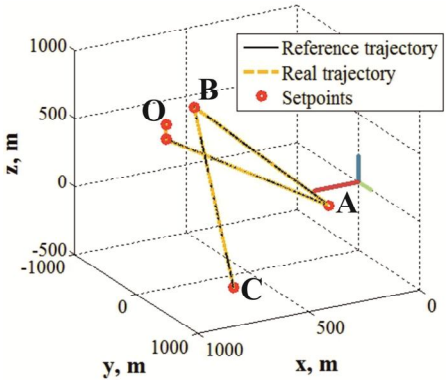

Fig. 5. Reference trajectory and realized trajectory while simulating research

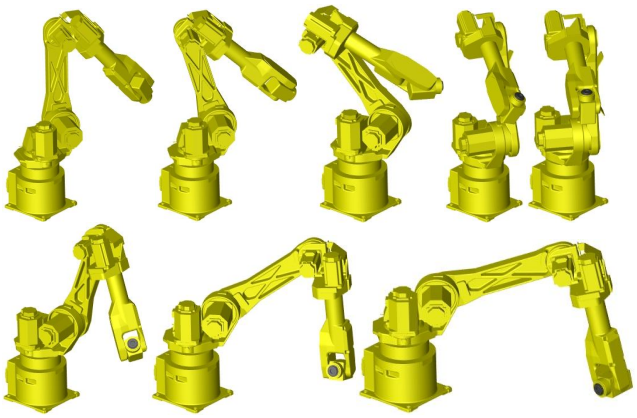

Fig. 6. The view of arms' positions during robot's movement along reference trajectory

Table 3. Set values of kinematic parameters of the robot's TCP point

Pt.	Time, s	Accel., mm/s^2	Decel., mm/s^2
A	-	-	-
B	2.4	5000	5000
C	2.4	5000	5000

4.2 Results of simulations

Based on the simulations' results, the plots of the kinematic parameters were performed (Fig. 7). Values of the kinematic parameters of the TCP point were transformed into setpoint signals in each joint by the use of inverse kinematic systems (Fig. 8). Based on the performed simulation of the robot's work, the total driving torques on the motors' shafts were obtained (Fig. 9), and then the values of the resultant and partial loads (Fig. 10), (Fig. 11), (Fig. 12).

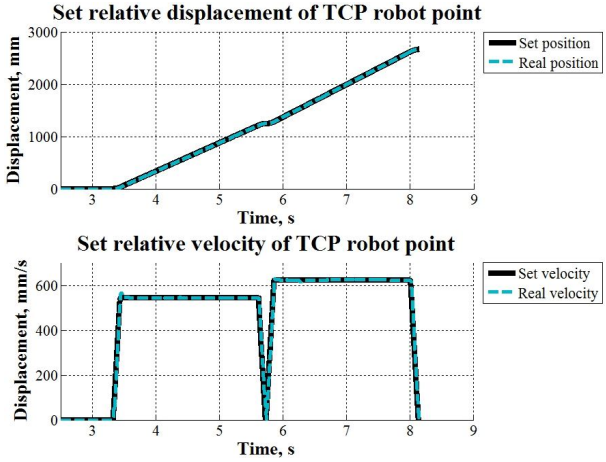

Fig. 7. The relative displacement and the speed profile of robot's TCP point

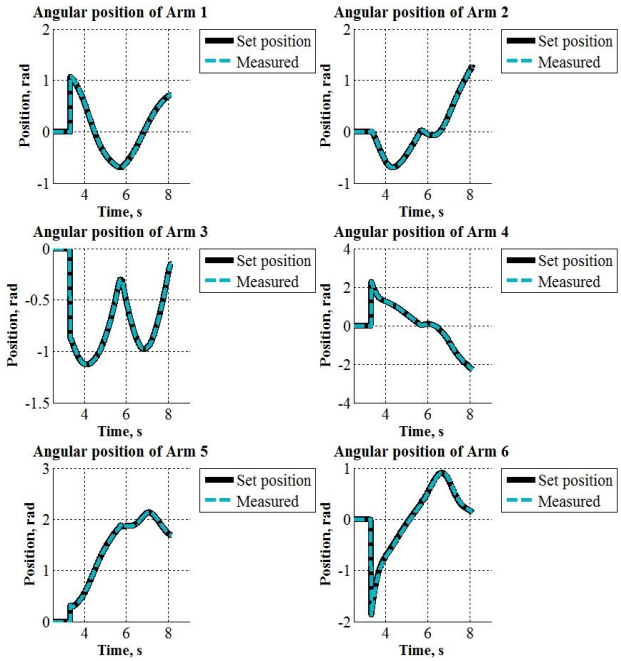

Fig. 8. Setpoint signal of arms' position

The numerical model calculated the driving torques by the use of the servo-control system. The values of the viscous friction were added to the results of the analytical model, thus obtaining the values of the total driving torque on the motors' shafts. Both driving torques obtained from numerical and analytical models were presented in one plot (Fig. 9).

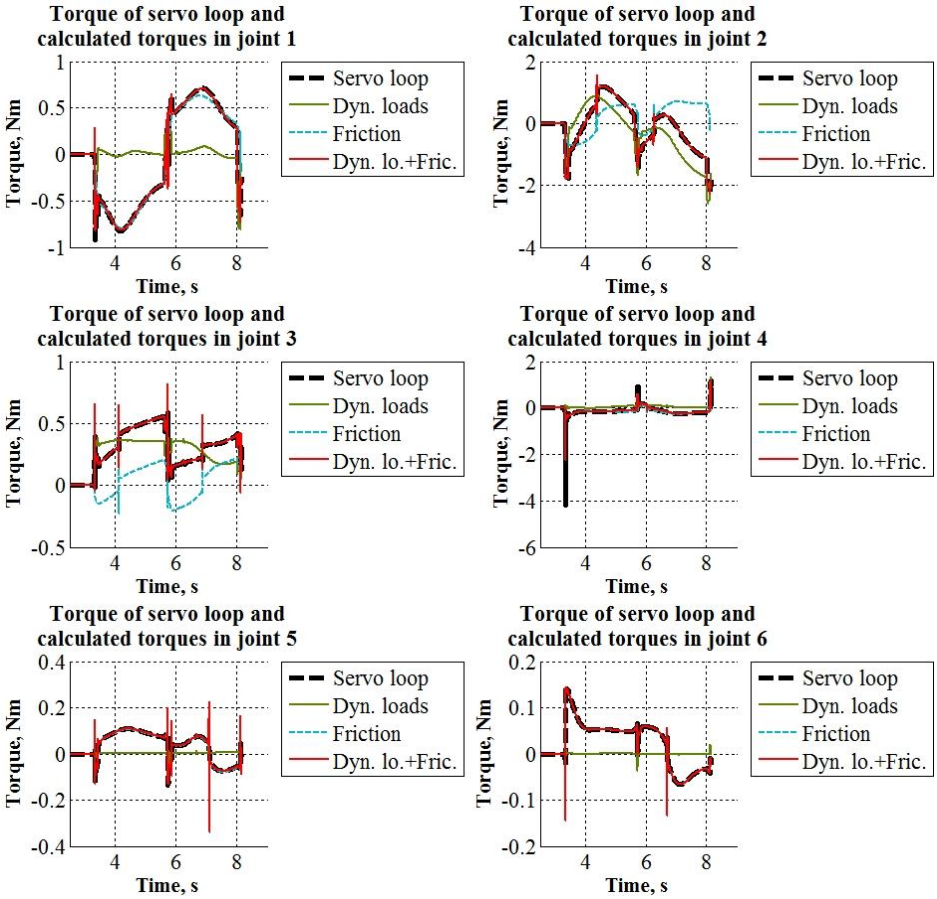

Fig. 9. The driving torques calculated numerically and analytically

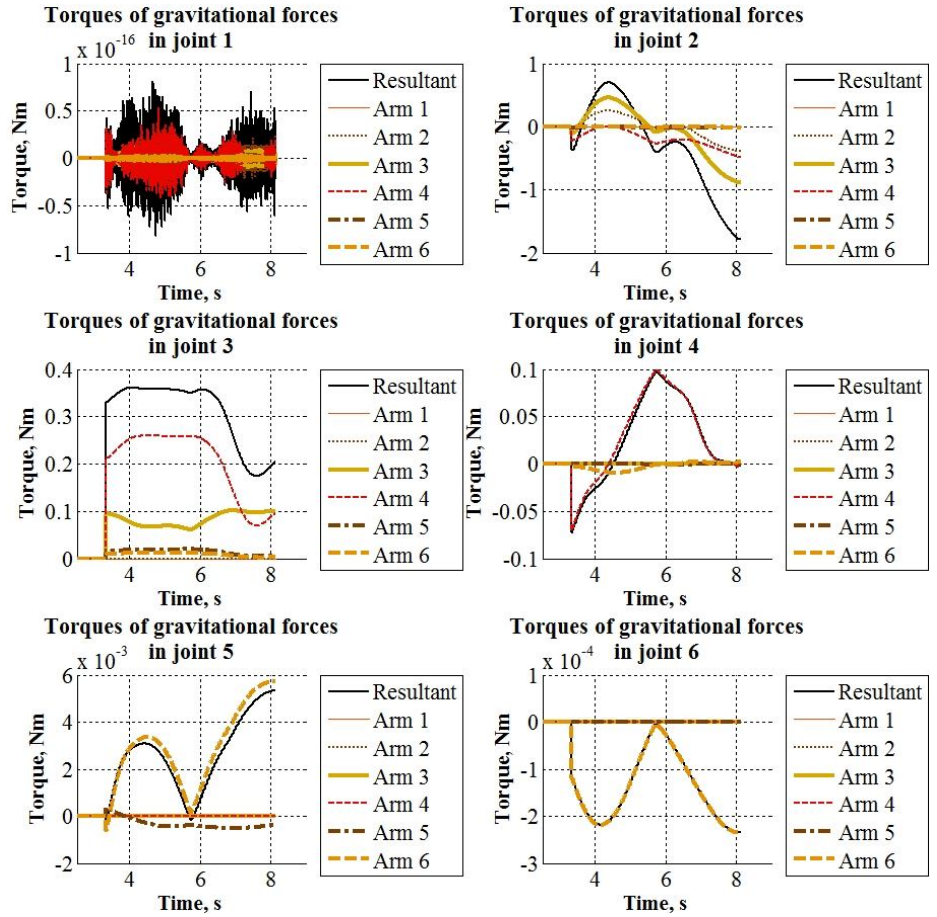

Fig. 10. Resultant and partial loads of motors' shafts results from gravitational forces

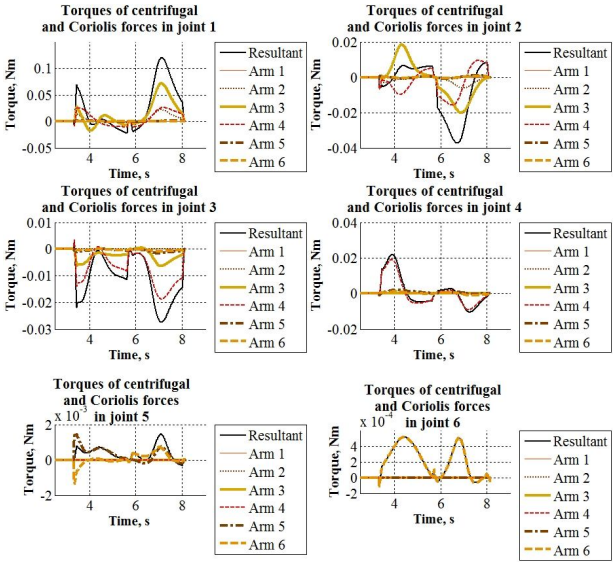

Fig. 11. Resultant and partial loads of motors' shafts results from centrifugal and Coriolis forces

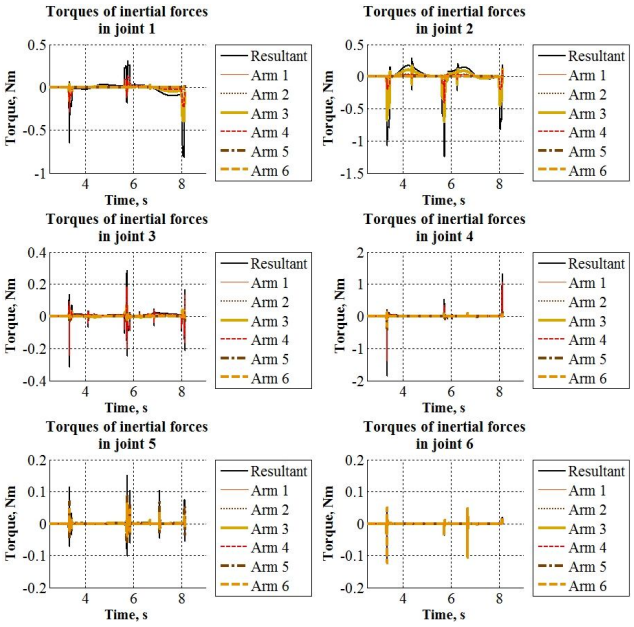

Fig. 12. Resultant and partial loads of motors' shafts results from inertial forces

10. CONCLUSIONS

The numerical and analytical models of the Fanuc AM100iB generate identical values of driving torques, as the result of setting the same input data of kinematic and dynamic parameters. It can therefore be regarded as confirmation of their full compliance and the correctness of their structure. Each model has its own advantages: the numerical model is used for visualisation of the robot's work in 3D space, in interactive mode and in real time, whilst the analytical model allowed for the performing of calculations of the resultant and partial loads acting on the motors' shafts. Both models will be used while simulating research into energy consumption by the investigated robot's drives. The resultant and partial loads will be used for the determination of the level of influence of selected forces on the total electric energy consumption in this type of machine. Selecting the most active loads will allow for this determination, which has to be taken into consideration during the process of energy consumption reduction.

11. ACKNOWLEDGEMENTS

The article was funded by the National Science Centre.
Decision number: DEC-2011/03/B/ST8/04631.

12. REFERENCES

1. Boyer, F., Coiffet, P., (1996), *Generalisation of Newton–Euler model for flexible manipulators*, International Journal of Robotic Systems, Vol. 13, No. 1, pp. 11-24.
2. Boyer, F., Coiffet, P., (1996), *Symbolic modelling of a flexible manipulator via assembling of its generalized Newton–Euler model*, Journal of Mechanism and Machine Theory, Vol. 31, pp.45–56.
3. Craig, J., (2005), Introduction to Robotics Mechanics and Control, pp. 62-100, Pearson Education, Incorporated, California.
4. Craig, J., (2005), *Introduction to Robotics Mechanics and Control*, pp. 171-178, Pearson Education, Incorporated, California] [Yoshikawa, T., (2003). *Foundations of robotics: Analysis and Control*, The MIT Press, pp.100-108.
5. Hollerbach, J. M., (1980), *A Recursive Lagrangian Formulation of Manipulator Dynamics and a Comparative Study of Dynamics Formulation Complexity*, IEEE Trans. Syst. Man and Cybern., Vol. SMC-IO, pp. 730-736.
6. Luca, A., Ferrajoli, L., (2009), *A modified newton-euler method for dynamic computations in robot fault detection and control*, Robotics and Automation, 2009. ICRA '09. IEEE International Conference, pp. 3359-3364, Roma.
7. Luh, J., Y. S., Walker, M. W., Paul, R. P., (1980), *On-line computational scheme for mechanical manipulator*, Trans. ASME J. Dynam. Syst. Mea. Contr., vol. 102, pp. 69-76.
8. Xiaogeng, He, Goldenberg, A. A., (1990), *An algorithm for efficient computation of dynamics of robotic manipulators*, Journal of Robotic Systems, pp. 689-702, Toronto.
9. Yoshikawa, T., (2003), *Foundations of robotics: Analysis and Control*, The MIT Press, pp.100-108.
10. Świder, J., Zbilski, A., (2013), *The Interactive Driving Profile Generation System*, Applied Mechanics and Materials, Vol. 307, No. 66, pp. 66-74.

Received: July 15, 2013 / Accepted: December 5, 2013 / Paper available online: December 10, 2013 © International Journal of Modern Manufacturing Technologies.